

PAPER • OPEN ACCESS

The role of zirconia additions on the microstructure and corrosion behavior of Ni-Cr dental alloys

To cite this article: Nawal Mohammed Dawood *et al* 2021 *Mater. Res. Express* **8** 045404

View the [article online](#) for updates and enhancements.



IOP | ebooks™

Bringing together innovative digital publishing with leading authors from the global scientific community.

Start exploring the collection—download the first chapter of every title for free.



PAPER

OPEN ACCESS

RECEIVED
9 February 2021REVISED
17 April 2021ACCEPTED FOR PUBLICATION
22 April 2021PUBLISHED
30 April 2021

Original content from this work may be used under the terms of the [Creative Commons Attribution 4.0 licence](#).

Any further distribution of this work must maintain attribution to the author(s) and the title of the work, journal citation and DOI.



The role of zirconia additions on the microstructure and corrosion behavior of Ni-Cr dental alloys

Nawal Mohammed Dawood , Kadhim F Al-Sultani and Hussein Hatem Jasim

Faculty of Materials Engineering, University of Babylon, Babylon, Iraq

E-mail: Mat.newal.mohammed@uobabylon.edu.iq

Keywords: NiCr, dental alloys, zirconium, powder metallurgy, corrosion

Abstract

This study investigates the effect of zirconia addition with different percentages on Ni-Cr alloy using a powder metallurgy technique. The scanning electron microscope with energy dispersive spectroscopy is used to analyze the microstructure of Ni-Cr and Ni-Cr-x ZrO₂ (where x is 3, 6, 9 wt.%) alloys. The x-ray diffraction method is used to determine the phases for Ni-Cr and Ni-Cr/ZrO₂ alloys. The corrosion and ion release tests were also achieved using potentiodynamic polarization and atomic absorption spectroscopy. According to the microstructural investigation, the results found that the Ni-Cr alloy's grain size tends to reduce with the addition of ZrO₂ with obtaining the smallest grain size with 6 wt.% addition. The potentiodynamic polarization exhibited that the modified alloys are more resistant to corrosion in the saliva medium than the Ni-Cr alloy. Furthermore, the role of ZrO₂ in dissolution test shows the development in the passive layer's resistance compared to unmodified alloys with reducing the Ni release from 2.5 ppm to 0.2 ppm. It can conclude that the addition of ZrO₂ has significantly improved Ni-Cr's biocompatibility and extend the area of implementations.

1. Introduction

Metal alloys have been used in various dental applications for many decades. Metal alloys are still common in the dental practice, and implants, such as bridge and porcelain-fused-to-metal (PFM) crowns due to their favorable mechanical properties and reasonable price [1, 2], despite being available in many non-metallic materials. However, chronic adverse reactions, for example, gingival pigments, gingival atrophy or hyperplasia, and urticaria have been reported with minor and significant allergic responses [3, 4]. Various risk factors, including the potential for cytotoxicity, must also be considered when carrying out biological assessments. Previous research on industrial alloys shows that continuous corrosion is typically due to multiple individual variables [5]. As a result, metals could be released from dental alloys as ions into surrounding tissues and saliva and then likely diffused across the body through the blood, causing possible cytotoxic effects for extended periods on local tissue or distant organs [6]. The biological impact or trace metals produced in peripheral blood and distant organ by dental alloys were studied extensively.

Jakobsen *et al* reported that metals released from the Co-Cr-Mo alloy accumulated in rats after nine months in the liver and kidney [7]. After six months in rabbits with Ni-Cr crowns, Zhu *et al* observed elevated Ni and Cr in blood [8]. In addition, McGinley and colleagues have shown that Ni can be the primary cause of cytotoxicity and apoptosis and that Ni's inhibitory effect is partly due to its ability to induce apoptosis via caspase-3 activation [9, 10]. Recent research about nickel-chromium alloy's possible toxicity on the kidneys has attracted much attention in China. This results in patients requesting the removal of dental restorations with heightened fears regarding dental alloys' safety.

Moreover, patients who have had PFM dental implants often need to get their implants replaced due to complications such as framework fractures and veneer chipping (such as caries and abutment tooth fracture) [11, 12]. The accumulation of trace metals and potentially harmful effects can be minimized or terminated by removing dental alloys needs examination. In dental applications, Ni-Cr alloys are used for long periods and

Table 1. Purity % and Average Particle Size of Materials.

Material	Purity%	Average particle size (μm)	Supplied company
Nickel powder (Ni)	99.93	70.55	Bucks Fluka AG Co. Germany
Chromium powder (Cr)	99.9	11.96	Fluka AG. Switzerland
Cobalt powder (Co)	99.61	17.28	Thomas Baker India
Molybdenum powder (Mo)	99.9	18.82	BDH Chemicals Ltd Poole England
Zirconia powder (ZrO_2)	99.9	17.34	E. Merck, Darmstadt

Table 2. Chemical composition of the prepared samples.

Alloy	Chemical composition (wt.%)	Alloy Code
Base alloy Ni-Cr Ni-Cr/ ZrO_2	75 Ni-21Cr- 2Co-2Mo	Ni-Cr
	72 Ni- 21Cr- 2Co-2Mo-3% ZrO_2	Ni-Cr-3 wt.% ZrO_2
	69 Ni- 21Cr- 2Co-2Mo-6% ZrO_2	Ni-Cr-6 wt.% ZrO_2
	66 Ni- 21Cr- 2Co-2Mo-9% ZrO_2	Ni-Cr-9 ZrO_2

substituted by patients who cannot be removed [13]. While the concentration of trace metals in dental patients is not proven to have any adverse effects, trace metals can be toxic and potentially affect primary biological and cellular functions. Therefore, information about the amounts of trace metals in distant organs affected by Ni-Cr dental alloys greatly benefits researchers. Furthermore, the Ni-Cr alloys' corrosion behavior properties mainly depend on forming the passive layer [11]. Therefore, the performance of the Ni-Cr alloys corrosion behavior in the dental applications is vital in order to understand their bio-characteristics and their compatibility are represented by the benefit-risks of the health of these alloys.

On the other hand, structural ceramics are widely used in medical implant applications as an efficient replacement for metallic dental prostheses' infrastructure. Zirconia is one of the best ceramics that emerged as a promising and multipurpose material to be used in several medical applications because of its excellent optical, mechanical, and biological properties [14, 15]. These properties have accelerated their path for CAD/CAM technology usage for several prosthetic treatment types [16]. Zirconia is defined as a biomaterial that showed a promising future due to its high fracture toughness and mechanical strength and the continuous advantages over other types of materials due to the mechanisms of the toughness transformation in their microstructural change [17].

However, the addition of ZrO_2 as the third element to the Ni-Cr alloy has yet been studied. Thus, this work investigates the effect of ZrO_2 addition, for three weight percentages, to Ni-Cr alloy. The ion releasing and corrosion behavior in artificial saliva are analyzed in order to discover the capacity of using the presented alloy as restorative materials.

2. Experimental procedures

2.1. Materials used

The materials used to prepare and reinforce the Ni-Cr alloys in this work were demonstrated in table 1 with average particle size, purity, and supplied company. The particle size was measured using a better size 2000 laser particle size analyzer and a handheld (XRF) analyzer type (DS-2000), USA, to determine powders' purity. The sample code and the detailed description of the prepared samples used in the present study are shown in table 2.

2.2. Powder mixing

The powders are mixed using the electrical rolling mixer type (STGQM-1/5-2). To ensure the mixing of powders, steel balls are used in different sizes with minimal alcohol added to eliminate the friction and oxidation generated during the mixing process for 6 h.

2.3. Powder compacting

In this stage, an electrical hydraulic press is used for compacting the blended powder to get green samples of 13 mm and 5 mm in diameter and thickness, respectively, to be used in the test. To reduce the friction resulting from the direct contact between the walls of the die and green compact, graphite powder was used as a lubricant. Graphite applications are also used to avoid the initiated cracks resulted from green compact ejection. The green

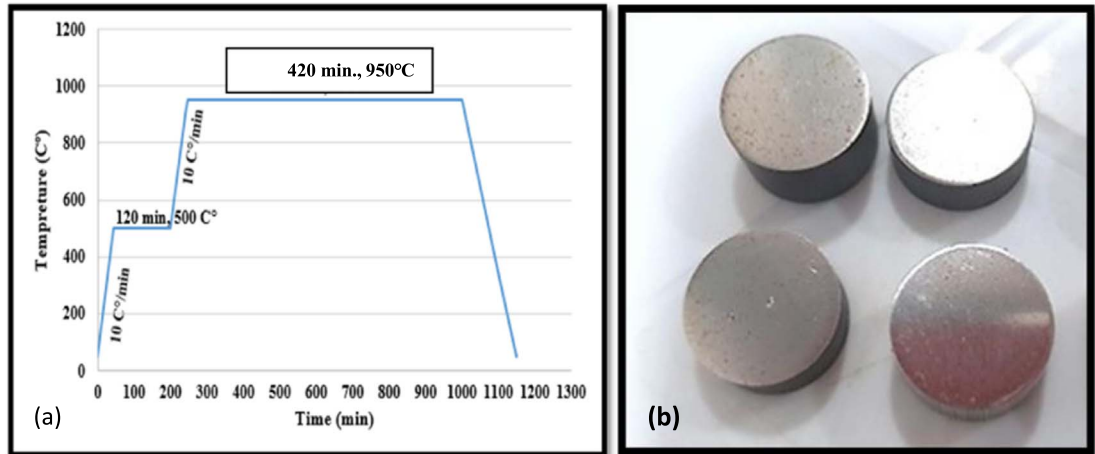


Figure 1. (a) Sintering process diagram and (b) sintered samples.

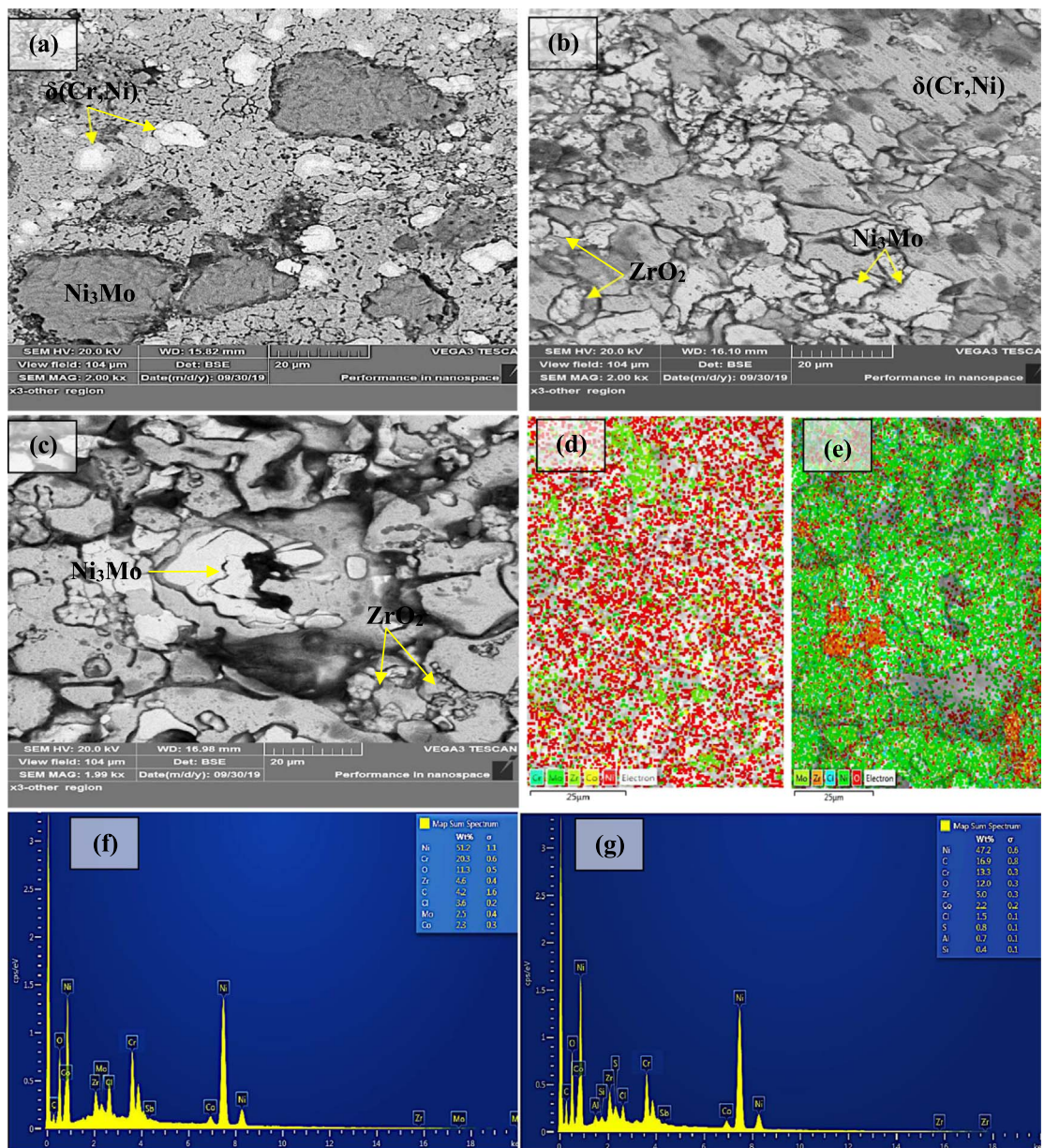


Figure 2. Microstructure analysis of the bare and modified alloys with different addition of ZrO₂, scanning electron microscopy of (a) Ni-Cr, (b) Ni-Cr-6 wt.% ZrO₂ and (c) Ni-Cr-9 wt.% ZrO₂; elemental mapping of (d) Ni-Cr-6 wt.% ZrO₂ and (e) Ni-Cr-9 wt.% ZrO₂; EDS spectrum analysis for (f) Ni-Cr-6 wt.% ZrO₂ and (g) Ni-Cr-9 wt.% ZrO₂.

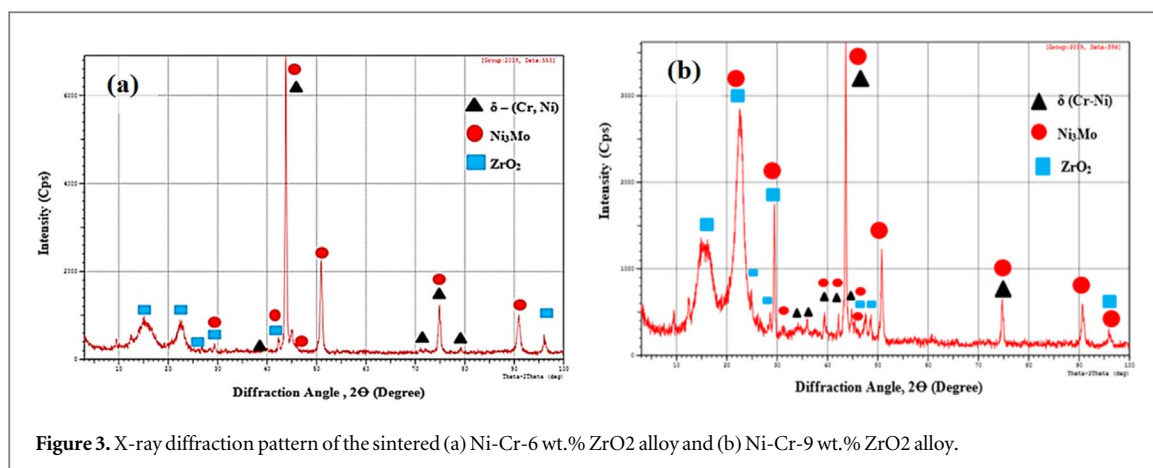


Figure 3. X-ray diffraction pattern of the sintered (a) Ni-Cr-6 wt.% ZrO₂ alloy and (b) Ni-Cr-9 wt.% ZrO₂ alloy.

Table 3. Chemical composition of etching solution [18].

No.	Constituent	ml
1	Nitric acid (1.40)	20
2	Hydrochloric acid (1.19)	20
3	Hydrogen peroxide (30%), concentration variable	10
4	Distilled water	Remain

compacted samples have been sintered in a vacuum tube furnace type: GSL 1600X/MTI. Figures 1(a) and (b) show the sintering process diagram and the final shape of sintered samples.

All samples were ground after sintering process utilizing grit silicon carbide papers of (180, 220, 320, 600, 800, 1000, 1200, 1500, 2000, and 2500), then they were polished utilizing a diamond past of 15 μm and metallographic polishing pads to obtain a bright mirror finishing finally. Etching at room temperature was conducted. Etching solution having a chemical composition listed in table 3 was used [18]. The samples were cleaned with water and dried after the etching process.

The phase analysis was performed using x-ray diffraction (XRD6000) with CuK α radiation at 40 kV and the scanning step of 5° per minute. The surface morphology and chemical analysis were characterized using (SEM, VEGA3 LM) equipped with INCA-AE350 Energy-dispersive x-ray spectroscopy (EDX).

The modified and unmodified alloy's corrosion characteristics were measured with Tafel test in an artificial saliva solution at 37 °C and 6.7 pH. The chemical composition of artificial saliva is illustrated in table 4 [19].

According to the ASTM standard, the Pt, SCE, and the sample were used as a counter, reference, and working electrodes, respectively. The potentiodynamic polarization curves were constructed. Using Tafel plots, the corrosion potential and corrosion current density (I_{corr}) were estimated by anodic and cathodic branches. The test was carried out with potential being stepped at scanning rate equals 0.4 mV s^{-1} from an initial potential that equals 250 mV below the potential of an open circuit. The scanning was continued up to 250 mV above the potentials of the open circuit. The measured rate of corrosion can be obtained as following [20, 21]:

$$\text{Corrosion rate (mpy)} = \frac{0.13 I_{\text{corr}} (Ew)}{\rho}$$

Where Ew , ρ , I_{corr} , mpy refer to the equivalent weight (g/eq.), density (g cm^{-3}), current density ($\mu\text{A cm}^{-2}$), and (mpy) (mils per year), respectively. The constant 0.13 represents the metric and time conversion factor.

According to [22], the Ni and Cr ions content leached into saliva from the samples was determined using dissolution tests to measure ions in sample solutions submerged at 37 °C for five weeks. A sample of each base alloy and modified with ZrO₂ samples were immersed in 50 ml of saliva in bottles made from polypropylene (PP). These bottles were closed firmly and incubated in the thermostatic chambers for five weeks at 37 °C. Every three days, the bottles were shaken quietly for a couple of seconds. After five weeks, the bottles' saliva and solution were analyzed using atomic absorption spectroscopy to determine the amount of Ni and Cr ions leached from each sample, according to Joan *et al* [23].

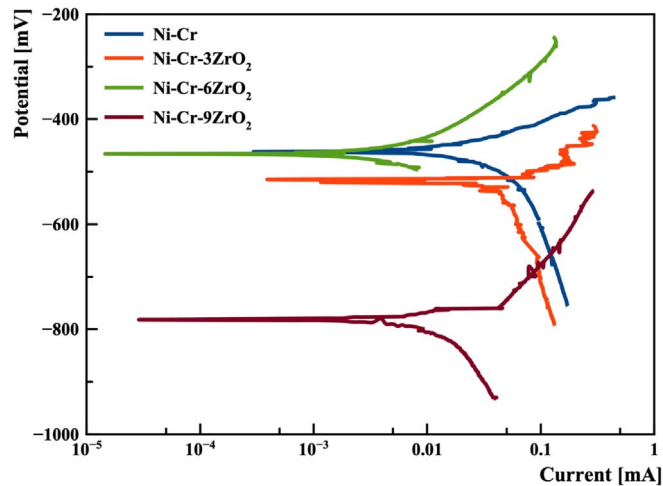


Figure 4. Potentiodynamic polarization for Ni-Cr alloy in synthetic saliva with and without ZrO₂ addition

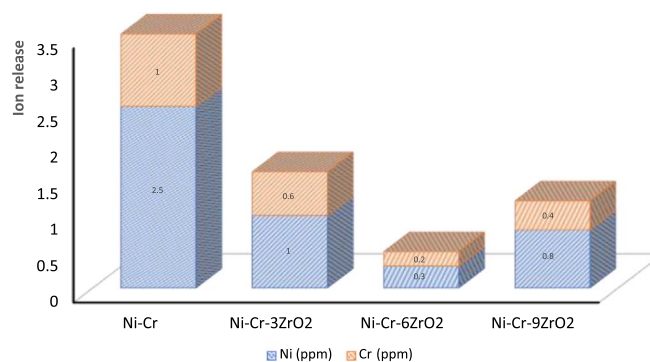


Figure 5. Ion release from samples immersed in synthetic saliva at 37 °C for 5 weeks.

Table 4. Chemical Composition of Artificial Saliva Solution [19].

Constituent in (g l ⁻¹)				
KCL	Na HCO ₃	NaH ₂ PO ₄ H ₂ O	HSCN	Lactic acid
1.5	1.5	0.5	0.5	0.9

3. Results and discussion

3.1. Microstructural observation

Figure 2 displays the SEM micrographs of the sintered modified and unmodified Ni-Cr alloys at 950 °C for seven hours. The results revealed that the sintered samples' microstructure of Ni-Cr- 6 wt.% ZrO₂ and Ni-Cr-9 wt.% ZrO₂ exhibited a structure with two phases; Ni₃Mo and ZrO₂ that formed in the matrix structure of δ (Cr, Ni). It was also clear that the sintered samples' grain size was obtained a smaller grain size with 6 wt.% of ZrO₂; further addition of ZrO₂ may increase the grain size. The alloying element of Ni, Cr, and Zr percentage addition was distributed uniformly in Ni-Cr's microstructure, as shown in the elemental mapping in figures 2(d) and (e). According to the EDX results (figures 2(f) and (g)), the percentage of the alloying element like Zr was varied according to the additional amount with identifying the percentage of oxygen, which shows an increase in the volume oxygen as the Zr addition increased from 6 wt.% to 9 wt.%. This is in good agreement with the elemental mapping in figures 2(d) and (e). The XRD scanning profile of the Ni-Cr-6 wt.% ZrO₂ and Ni-Cr-9 wt.% ZrO₂ alloys after been sintered at 950 °C for 7 h are shown in figures 3(a) and (b). The presentence peaks were reflected in the alloying formation rather than elements, in which it is proven that the 7 h sintering was sufficient enough

Table 5. The corrosion current (I_{corr}), corrosion potential (E_{corr}), and the corrosion rate for all used alloys in synthetic saliva solution at 37 °C.

Sample code	Current density, i_{corr} ($\mu\text{A cm}^{-2}$)	The corrosion potential, E (mV)	Cathodic slope, β_c (mV)	Anodic slope, β_a (mV)	Corrosion rate, (mpy)
Ni-Cr	4.51	-531.4	28.7	12.3	73.28
Ni-Cr-3ZrO ₂	0.20	-461.1	44	41.7	3.25
Ni-Cr-6ZrO ₂	0.03	-475.4	30.1	30.3	0.487
Ni-Cr-9ZrO ₂	0.09	-784.1	43.6	38.3	1.462

to complete the transformation. On the other hand, forming the alloying compounds rather than individual elements reduces the toxicity effect into the body as a future biomaterial's implementations [24]. Furthermore, the observed Ni₃Mo and δ (Ni-Cr) phases' peak intensity tends to increase as ZrO₂ addition increased.

3.2. Porosity and density after sintering

The porosity and density of Base alloy Ni-Cr and Ni-Cr-3, 6, and 9 wt. % ZrO₂ after sintering have been determined according to the ASTM B-328 standard [25]. Final porosity is the measuring for closed and open pores in the volume sintered samples. The porosity of the base alloy is 16.21 % and this represents the open and closed pores in the sample. It was noticed that ZrO₂ addition decrease the porosity value to 13.46, 11.21, and 10.96% with 3, 6, and 9 wt. % ZrO₂ addition respectively due to the small particle size of zirconia that can move and full the spaces between the settled particles during compaction which gives lower porosity after the sintering process. The presence of pores decreases the strength because the pores act as stress concentration regions and crack initiation regions also affect the corrosion resistance of the alloy because the pores may extend to the internal surface and increase the corrosion occur due to increasing the surface area [26, 27]. The existence of ZrO₂ addition leads to an increase in the contact areas between the particles, however, this will increase the diffusion between the particles in the sintering process which leads to a decrease in the porosity and increase the density. It was observed that the density of sintered sample for the Base alloy Ni-Cr is 8.012 g cm⁻³ and for Ni-Cr-3, 6, and 9 wt. % ZrO₂ are 8.246, 8.692, and 8.842 g cm⁻³.

3.3. Potentiodynamic polarization

Figure 4 presents the potentiodynamic polarization curves of Ni-Cr alloy without and with ZrO₂ addition of in synthetic saliva solution at 37 °C. The corrosion parameters, such as corrosion potential, corrosion current, polarization constant (β_c, β_a), and corrosion current densities, were extracted from these curves and tabulated in table 5. It can be observed that there is a significant shift toward lower current densities of the polarization curves for the sample with different additives of ZrO₂. The I_{corr} for the Ni-Cr-3 wt.% ZrO₂ is around 0.20 $\mu\text{A cm}^{-2}$, while, I_{corr} for Ni-Cr-6 wt% ZrO₂ and Ni-Cr-9 wt% ZrO₂ is around 0.03 $\mu\text{A cm}^{-2}$ and 0.09 $\mu\text{A cm}^{-2}$, respectively, which are much lower than I_{corr} for the bare alloy, which around 4.51 $\mu\text{A cm}^{-2}$. These results indicate the stability of the Cr₂O₃ passive layer against dissolution, and these findings are in agreement with another research in [28]. The corrosion current and the calculated corrosion rate are relative measurements of corrosion, and they refer to the material loss magnitude throughout the corrosion process. Therefore, the higher current density and the calculated corrosion rate cause more materials to lose [28]. In Ni-Cr alloys, Cr plays a crucial role in protecting the surface via forming a Cr₂O₃ layer that leads to passive these alloys. However, corrosive ions in saliva can destroy such passive layers.

On the other hand, the results also revealed that the Ni-Cr with 3, 6, and 9 wt.% ZrO₂ alloys are achieved a lower corrosion rate compared with the Ni-Cr alloy. This enhancement may attribute to the addition of ZrO₂ to the base alloy leads to corrosion potential (E_{corr}) shifting towards the active direction with a reduction in the density of the corrosion current, specifically in the existence of 6 and 9 wt% ZrO₂

3.4. Ni and Cr ions release measurement

Ni's ion's release may further stimulate nickel sensitization or provoke allergic contact dermatitis [29]. The Ni ions test release is applied to ensure that Ni-Cr alloys can be used in human bodies. Figure 5 illustrate Ni and Cr ions' concentration for the Ni-Cr alloys with and without ZrO₂ additions after five weeks of immersion in synthetic saliva at a temperature of 37 °C. Measurable released ions of Ni from the based alloy of Ni-Cr is about 2.5 ppm, and this amount led to decreased as the ZrO₂ was added with obtaining the minimum value of 0.3 ppm with 6 wt.% of ZrO₂. This improvement may be attributed to the ability of ZrO₂ to be incorporated with Ni in the matrix to reduce the metal dissolution and then permits for Cr₂O₃ to be continued.

However, the Cr ion releases, shown in figure 5, indicate the highest percentage of Cr ion release with Ni-Cr's unmodified alloy. The release amount reduced as the ZrO₂ addition increase with an optimum value of 0.2 ppm with 6 wt.% addition, and as the ZrO₂ increased to 9 wt.%, the ion release of Cr tends to increase as well. On the

other hand, the results also revealed that the release of Cr from the Ni-Cr alloy was much lower than the Ni release in artificial saliva, which may attribute to Cr's lower content in the Ni-Cr alloy composition. In general, releasing any element increased as its percentage in the alloy is increased [30]. In addition, the Ni-Cr alloy's corrosion properties depend on their bulk composition, the protective surface oxide microstructure, and its development [29]. Despite this, the ZrO₂ existence as cathodic regions reduces the Ni and Cr dissolution from the alloy and, therefore, eliminates the rate of corrosion and thus increases the Cr₂O₃ passive layer's presence.

4. Conclusions

Based on the obtained results, the following conclusions were drawn:

1. The Ni-Cr alloy's grain size was tending to decrease as the ZrO₂ addition increase with exhibiting the smallest grain size with 6 wt.% addition; however, with a further addition to 9 wt.%, the grain size actually increased.
2. The Ni-Cr alloy's corrosion rate reduced from 73.28 mpy to 0.487 mpy as the ZrO₂ was added with an optimum percentage of 6 wt.%.
3. Ni and Cr's highest ion release was obtained with the unmodified alloy with 2.5 ppm and 1 ppm, respectively. Conversely, the addition of ZrO₂ with 6 wt.% presented the lowest ion release with an average value of 0.3 ppm and 0.2 ppm for the Ni and Cr, respectively.

ORCID iDs

Nawal Mohammed Dawood  <https://orcid.org/0000-0002-3610-5491>

References

- [1] Koizumi H et al 2019 Application of titanium and titanium alloys to fixed dental prostheses *Journal of Prosthodontic Research* **63** 266–70
- [2] Wataha J C 2002 Alloys for prosthodontic restorations *The Journal of Prosthetic Dentistry* **87** 351–63
- [3] Mittermüller P et al 2018 Five hundred patients reporting on adverse effects from dental materials: frequencies, complaints, symptoms, allergies *Dent. Mater.* **34** 1756–68
- [4] Kitagawa M et al 2019 Current status of dental metal allergy in Japan *Journal of Prosthodontic Research* **63** 309–12
- [5] Geurtsen W 2002 Biocompatibility of dental casting alloys *Critical Reviews in Oral Biology & Medicine* **13** 71–84
- [6] Siddharth R et al 2015 Quantitative analysis of leaching of different metals in human saliva from dental casting alloys: an *in vivo* study *The Journal of the Indian Prosthodontic Society* **15** 206
- [7] Jakobsen S S et al 2007 Cobalt-chromium-molybdenum alloy causes metal accumulation and metallothionein up-regulation in rat liver and kidney *Basic Clin. Pharmacol. Toxicol.* **101** 441–6
- [8] Zhu G et al 2004 Analysis on content of Ni-Cr in gingival and blood of hares after wearing non-noble porcelain-fused-to-metal crown *Hua xi kou qiang yi xue za zhi = Huaxi kouqiang yixue zazhi = West China Journal of Stomatology* **22** 284–6
- [9] McGinley E L, Moran G P and Fleming G J 2013 Biocompatibility effects of indirect exposure of base-metal dental casting alloys to a human-derived three-dimensional oral mucosal model *Journal of Dentistry* **41** 1091–100
- [10] Pan Y et al 2017 Cell death affected by dental alloys: Modes and mechanisms *Dental Mater. J.* **36** 82–7
- [11] Zheng C et al 2020 Corrosion behavior of a Ni-Cr-Mo alloy coating fabricated by laser cladding in a simulated sulfuric acid dew point corrosion environment *Coatings* **10** 849
- [12] Spies B C et al 2017 All-ceramic, bi-layered crowns supported by zirconia implants: three-year results of a prospective multicenter study *Journal of Dentistry* **67** 58–65
- [13] Furrer S et al 2018 Metal hypersensitivity in patients with orthopaedic implant complications—a retrospective clinical study *Contact Dermatitis* **79** 91–8
- [14] Galante R, Figueiredo-Pina C G and Serro A P 2019 Additive manufacturing of ceramics for dental applications: a review *Dent. Mater.* **35** 825–46
- [15] Schünemann F H et al 2019 Zirconia surface modifications for implant dentistry *Materials Science and Engineering: C* **98** 1294–305
- [16] Memari Y et al 2019 Marginal adaptation of CAD/CAM all-ceramic crowns made by different impression methods: a literature review *Journal of Prosthodontics* **28** e536–44
- [17] Rehman M, Madni A and Webster T J 2018 The era of biofunctional biomaterials in orthopedics: what does the future hold? *Expert Review of Medical Devices* **15** 193–204
- [18] Petzow G 1999 *Metallographic Etching, 2nd Edition: Techniques for Metallography, Ceramography, Plastography* (ASM International)
- [19] Rajih A, Dawood N and Rasheed F 2018 Corrosion protection of 316L stainless steel by HA coating via pulsed laser deposition technique *J. of Eng. and App. Sci.* **13** 10221–31
- [20] Bakhsheshi-Rad H et al 2016 Structure, corrosion behavior, and antibacterial properties of nano-silica/graphene oxide coating on biodegradable magnesium alloy for biomedical applications *Vacuum* **131** 106–10
- [21] Saud S N et al 2016 Corrosion and bioactivity performance of graphene oxide coating on TiNb shape memory alloys in simulated body fluid *Mater. Sci. Eng. C* **68** 687–94
- [22] Reclaru L et al 2012 Ni-Cr based dental alloys; Ni release, corrosion and biological evaluation *Materials Science and Engineering: C* **32** 1452–60
- [23] Loch J et al 2015 Electrochemical behaviour of Co-Cr and Ni-Cr dental alloys *Solid State Phenomena* (Trans Tech Publ.)

- [24] Atiyah A A, Ali A-R K A and Dawood N M 2015 Characterization of NiTi and NiTiCu porous shape memory alloys prepared by powder metallurgy (Part I) *Arab. J. Sci. Eng.* **40** 901–13
- [25] ASTM B328-96(2003)e1, Standard Test Method for Density, Oil Content, and Interconnected Porosity of Sintered Metal Structural Parts and Oil-Impregnated Bearings (Withdrawn 2009)
- [26] Brodnikovskii N P 2003 Properties of Ni–Cr–Al Alloys Obtained by a Powder Metallurgy Method *Powder Metall. Met. Ceram.* **42** 137–44
- [27] Lamiaa Z M *et al* 2020 Characteristics of Ni-Cr binary alloys produced by conventional powder metallurgy *Key Eng. Mater.* **835** 214–22
- [28] Da Silva L J *et al* 2017 Effect of casting atmosphere on the marginal deficiency and misfit of Ni-Cr alloys with and without beryllium *The Journal of Prosthetic Dentistry* **118** 83–8
- [29] Liliana P *et al* 2018 Corrosion behavior of Ni-Cr dental casting alloys *Int J Electrochem* **13** 410- 423
- [30] Al-Jmmal A Y 2014 Metal ion release from Ni-Cr alloy with different artificial saliva acidities *Al-Rafidain Dental Journal* **14** 266–71